Space dispersion feature of the conduction electron spin resonance in two-dimensional electron systems caused by the absence of 'up-down' symmetry



1993 J. Phys.: Condens. Matter 5 2603

(http://iopscience.iop.org/0953-8984/5/16/017)

J. Phys.: Condens. Matter 5 (1993) 2603–2618. Printed in the UK

# Space dispersion feature of the conduction electron spin resonance in two-dimensional electron systems caused by the absence of 'up–down' symmetry

V M Edelstein

Institute of Solid State Physics, Russian Academy of Sciences, Chernogolovka, Moscow Region 142432, Russia

Received 23 January 1992, in final form 24 July 1992

**Abstract.** The conduction electron spin resonance (CESR) in two-dimensional (2D) electron systems (inversion layers of semiconductor heterostructures and quantum wells) without 'up–down' symmetry is considered. The pyroelectric-like symmetry of such a layer makes a difference between two normals to the layer and thus leads to the 2D-electron Hamiltonian which includes an additional spin–orbit term $H_{so} = (\alpha/\hbar)(\boldsymbol{p} \times \boldsymbol{c}) \cdot \boldsymbol{\sigma}$, where $\boldsymbol{c}$ is the vector of one of the non-equivalent normals. Accurate quantum kinetic theory with regard for the spin–orbit energy is proposed for the first time, and the paramagnetic linear response is evaluated. It is shown that, if the CESR is excited by a wave of wavevector $\boldsymbol{q}$, then the decay rate should include a term which reverses its sign with an applied magnetic field $\boldsymbol{B}$ reversal and, for $\boldsymbol{B}$ parallel to the plane of electron motion, is given by

$$\Gamma = (\hbar/\tau)[3(\alpha p_F \tau/\hbar^2)^2 + \tfrac{1}{2}(v_F \tau q)^2 + 2\alpha m v_F^2 \tau^2 \hbar^{-2} \boldsymbol{q} \cdot (\boldsymbol{c} \times \hat{\boldsymbol{B}})]$$

where $\tau$ is the mean collision time and $v_F$ is the Fermi velocity. An estimate for the effect in some semiconductor heterostructures is presented, and possibilities of experimental observation are briefly discussed.

## 1. Introduction

After the discovery of optical activity by Arago in 1811 and Biot in 1812, considerable attention was paid to the study of physical systems with violated space parity for uncommon properties that could reveal such objects. Recently, an analogy of parity violation has been observed in two-dimensional (2D) electronic systems. For the first time, speculations about this were initiated by experiments on $GaAs/Al_xGa_{1-x}As$ heterostructures [1]. Linear extrapolation of electron spin resonance energies measured at a finite magnetic field to $\boldsymbol{B} = \boldsymbol{0}$ gave rise to a finite spin splitting of the conduction band. This phenomenon was interpreted as the existence of a spin–orbit interaction induced by parity violation with respect to reflection in the plane of the 2D electron layer. In [2] it was proposed to describe the situation phenomenologically by adding to the carrier-effective-mass Hamiltonian a spin–orbit (SO) term (the Rashba term) of the form

$$H_{so} = (\alpha/\hbar)(\boldsymbol{p} \times \boldsymbol{c}) \cdot \boldsymbol{\sigma} \tag{1.1}$$

where $\boldsymbol{p}$ is the electron 2D momentum operator, $\boldsymbol{\sigma}$ is the Pauli matrix vector and $\boldsymbol{c}$ is the unit vector normal to the layer. However, another reason for lifting the spin degeneracy,

0953-8984/93/162603+16$07.50  

based on the lack of inversion symmetry in the elementary cell of the bulk GaAs crystal (the $p^3$-term), was soon discovered. Subsequent calculations [3] and measurements [4] led to the conclusion that the Rashba term is apparently small in GaAs but should dominate in narrow-band-gap semiconductors, such as InAs. Indeed, the zero-field splitting in $In_xGa_{1-x}As/In_yAl_{1-y}As$ [5] and GaSb/InAs [6] heterostructures has also been deduced from an analysis of the beat pattern observed in Shubnikov–de Haas oscillations at high magnetic fields. The results of the experiments were successfully described with the help of the Rashba term and the value of the SO constant $\alpha/\hbar(In_xGa_{1-x}As/In_yAl_{1-y}As) \simeq 1.46 \times 10^{-10}$ eV cm and $\alpha/\hbar(GaSb/InAs) \simeq 0.9 \times 10^{-9}$ eV cm was evaluated. Note that the constant $\alpha$ of a 3D CdS crystal of polar symmetry has a fairly similar value: $\alpha/\hbar(CdS) \simeq 1.6 \times 10^{-10}$ eV cm [7].

For interpretation of the first experiments which revealed the spin-split character of the conduction band [1, 5, 6], one needed to know only the electron energy levels. More recently, the investigation of the spin-dependent physics of 2D electron structures has taken a new direction. A variety of kinetic phenomena, such as the weak localization [4] and the spin relaxation of electrons injected into the edge channel of a 2D electron gas in the quantum Hall regime [9], have appeared in the literature. All these phenomena need an accurate kinetic theory. So, for example, an attempt to understand and describe quantitatively weak-localization effects caused by a band SO interaction (the Rashba or the $p^3$ mechanism) with the help of formulae derived for the case of the impurity SO interaction (the Elliott [10] mechanism) is apparently useful but not quite correct.

The main obstacles to developing a rigorous kinetic theory for a system with SO coupling, regardless of its origin, relate to a non-trivial spin–momentum dependence acquired by scattering amplitudes, vertices and other attributes of such a theory. The present consideration avoids some of these mathematical complications by accepting the simplifying assumption that the impurity potential is of short-ranged character. However, the spin–momentum correlations due to the band SO interaction are completely retained. Owing to the novel form of identities for the tensor product of the Pauli matrices it appears to be possible to solve the transport equations without losing their spinor structure. Although identities of that kind are well known [11], the present form, in my opinion, is much more convenient for applications. The identities could be useful for any quantum theory of spin-dependent phenomena where because of the SO or exchange interaction the spinor structure of various processes plays a real role. In particular, it is not difficult to consider with their help the case of the $p^3$-type SO coupling which takes place in semiconductor structures based on GaAs crystals.

The main purpose of this study is to investigate the conduction electron spin resonance (CESR) in a 2D electron layer with destroyed reflection parity. We shall assume that the number of carriers in the layer is large enough to form a degenerate Fermi gas and study the hydrodynamic regime, where both the Larmor frequency $\omega_s = \mu_B g B$ and the driving frequency $\omega$ are low. Here $\mu_B$ is the Bohr magneton and $g$ is the Landé factor. A spin relaxation of the electrons within the model considered takes place through the Dyakonov–Perel [12] process; the SO energy (1.1) can be considered as the Zeeman energy in a fictitious magnetic field $\boldsymbol{B}_f(\boldsymbol{p}) = \alpha(\boldsymbol{p} \times \boldsymbol{c})/\mu_B g$ which stochastically changes its direction by impurity scattering, giving rise to the spin relaxation. In [12], only the uniform limit was considered provided that impurity broadening $\hbar/\tau$ is much larger than the spin-splitting energy $\alpha p_F/\hbar$ at the Fermi momentum $p_F$ and the spin relaxation time

$$\tau_s^{-1} \simeq \tau^{-1}(\alpha p_F \tau/\hbar^2)^2 \tag{1.2}$$

was found. It will be shown below that under the same condition

$$\alpha p_F \tau/\hbar^2 \ll 1 \tag{1.3}$$

the decay rate of non-uniform spin density of the wavevector $q$ should be a sum of three terms:

$$\tau_s^{-1}(q) = \tau^{-1}\{\tfrac{1}{4}\eta^2[3-(c\cdot\hat{B})^2] + \tfrac{1}{2}ql^2 + \eta l q\cdot(c\times\hat{B})\} \tag{1.4}$$

where $\eta = 2\alpha p_F\tau/\hbar^2$, $l = v_F\tau$ is the electron mean free path and $B$ is the applied magnetic field. Here the first term yields the relaxation of the uniform spin density and the second describes the usual diffusion. The extra term proportional to the invariant $q\cdot(c\times B)$, i.e. odd in the field $B$, the layer orientation $c$ and the wavevector $q$, represents a novel effect—a spin precession induced by diffusion. Some arguments for the interpretation will be presented in section 3 (see the text below equation (3.8)). For the first time such a term was predicted on the grounds of qualitative arguments and measured in a 3D CdS crystal in a remarkable paper [7]. However, to my knowledge, an attempt to deduce the term in the framework of a microscopic transport theory has never been reported before. The approach of [7] in the case under consideration would lead to an incorrect numerical pre-factor in the third term as well as loss of the angular dependence of the first term in equation (1.4). Unfortunately, equation (1.4) in the particular case of $B\perp c$ was stated in my previous paper [8] erroneously. To obtain the correct result, one should substitute $2\alpha$ for $\alpha$ in equation (4.3) of [8]. It should be emphasized that, although the SO constant $\alpha$ enters both the first and the third terms of equation (1.4), it might appear to be difficult to infer its value from measurement of the uniform spin-density relaxation because of other possible sources of the relaxation, for instance paramagnetic impurities, which are totally unrelated to the absence of reflection parity. It is the presence of the invariant $q\cdot(c\times B)$ that undoubtedly indicates the lack of 'up–down' symmetry of the 2D electronic system. The appearance of the $q\cdot(c\times B)$ dependence is typical of systems of polar symmetry. A correction of this type to the energy of excitons in a CdS crystal was first discovered in [13, 14] and called the 'magneto-Stark effect'.

The basic quantity to be calculated is the paramagnetic susceptibility tensor $\chi_{ij}(\omega, q)$. In principle, there are several possibilities for measuring the susceptibility. The imaginary part of $\chi_{ij}(\omega, q)$ can be inferred from the diffusion scattering cross section of neutrons (see [15], equation (8.69)) although, for neutron scattering, the small-$q$ process is usually difficult to observe because of the underlying Bragg peaks from lattice structure. For semiconductor quantum wells, the spin-flip Raman scattering might turn out to be a more sensitive method of studying $\chi_{ij}(\omega, q)$ (see [16], equation (2.92), and [17], equation (3.16)), in view of the fact that resonance enhancement of the scattering amplitude can be achieved.

Let us discuss experimental conditions for observing the CESR anomalous dispersion. For the $In_xGa_{1-x}As/In_yAl_{1-y}As$ heterostructure, which may be considered as a typical example, Das *et al* [5] measured the effective mass $m = 0.046m_0$, $\alpha/\hbar = 1.4\times10^{-10}$ eV cm so that the SO splitting of the Fermi surface $2\alpha k_F$ at the electron density $n_s \simeq 1\times10^{12}$ cm$^{-2}$ is equal to 0.65 meV. The SO coupling (1.1) determines a characteristic scale of wavevector $q_{so} = \alpha m/\hbar^2$ which for this case equals $0.96\times10^4$ cm$^{-1}$. To obtain a CESR narrow enough to be observed, one needs to fabricate a fairly dirty heterostructure, for instance with impurity broadening $\hbar/\tau \simeq 5$ meV, which is still appreciably smaller than the electron Fermi energy $\epsilon_F = \hbar^2k_F^2/2m \simeq 40$ meV. Then one would have $\eta = 0.13$, $\hbar/\tau_s(q=0, \hat{B}\perp c) = 0.064$ meV and, hence, $\omega_s\tau_s = 3$ at $B = 1.1$ T and $g \simeq 3$. Further, the ratio of the anomalous third term of equation (1.4) to the first term equals $4q/3q_{so}$ and the ratio of the second diffusion term to the third equals $q/2q_{so}$. By inelastic

scattering of infrared light of energy $\omega_I \simeq 0.5$ eV the scattering wavevector $q = k_I - k_S$ ($k_I$ and $k_S$ are the wavevectors of the incident and scattered light, respectively) ranges over an interval $0 \leqslant q \leqslant 2k_I \simeq 0.5 \times 10^5$ cm$^{-1}$. It can now be seen that a situation when all three terms of equation (1.4) are approximately equal could be realized.

Note that many of the ideas under discussion concerning the kinetics of conducting media with violated space parity are analogous to those of [18] in which some kinetic problems of metals containing non-centrosymmetric impurities were touched on.

The outline of this paper is the following. In section 2, a detailed description of the model and the Feynman rules are given. In section 3, a method for solution of the transport equation is presented. Evaluation of the paramagnetic susceptibility is performed in section 4. Some comments about the results obtained as well as the related problems are given in section 5. Appendix 1 contains a list of the identities for the tensor products of the Pauli matrices; appendix 2 demonstrates the technique of working with Feynman graphs; appendix 3 supplies necessary details for solving the transport equations.

It will be assumed below that the reader is familiar with the many-body quantum-field theory (the Matsubara method, the Feynman diagram technique, etc). For a review on these topics we refer to the textbook by Abrikosov *et al* [19] and the paper by Siegel [20]. A somewhat different formulation of some spin-dynamics problems in the Feynman diagram language can be found in the review by Barnes [21].

## 2. Model and formulation

Suppose that the degenerate Fermi gas of non-interacting electrons of charge $e$, spin $\frac{1}{2}$ and magnetic moment $\mu = -g\mu_B\sigma/2$ is subjected to an external static magnetic field $B$. Then the 'in-plane' Hamiltonian of the system under consideration has the form

$$H = H_0(p) + H_Z + H_{imp} \tag{2.1}$$

where

$$H_0(p) = p^2/2m + \alpha(p \times c) \cdot \sigma \tag{2.2}$$

$$H_Z = -\mu \cdot B \tag{2.3}$$

$$H_{imp} = \sum_i U\delta(r - R_i). \tag{2.4}$$

Here $r$ is the position of the electron and $R_i$ are the positions of the arbitrarily distributed short-range impurities of concentration $n_{imp}$. In equations (2.1)–(2.3) and in all equations below we set $\hbar = 1$.

There are several dimensionless parameters determining the dynamics and kinetics of the system. The applied magnetic field appears in the theory through two parameters which are treated below as small:

$$\omega_c\tau \ll 1 \qquad \omega_s\tau \ll 1 \tag{2.5}$$

where

$$\omega_c = |e|B/mc \qquad \omega_s = |g|\mu_B B \tag{2.6}$$

are the cyclotron and paramagnetic resonance frequencies, and $\tau$ is the mean scattering time given by

$$\tau^{-1} = mn_{\text{imp}}|U|^2. \tag{2.7}$$

One can show that the effect of diamagnetic quantization on the CESR is negligible at $\omega_c\tau \ll 1$ and $\eta^2 \ll 1$. The SO constant $\alpha$ also appears in the problem in two ways. The parameter $\delta = \alpha k_F/\epsilon_F$, $\epsilon_F = k_F^2/2m$, having to some extent a pure quantum mechanical nature is treated as being very small so that all powers of $\delta$ in equations in excess of the first can be ignored. Another parameter $\eta = 2\alpha k_F\tau$ controls the kinetics of spin-flip processes by impurity scattering. In this paper we adopt $\eta \ll 1$, i.e.

$$\delta \ll \eta \ll 1 \tag{2.8}$$

although, within the technique used, the parameter $\eta$ is allowed to take any value. The left-hand side of equation (2.8) means that

$$k_F l \gg 1 \tag{2.9}$$

where $l = v_F\tau$ is the mean free path and $v_F = k_F/m$ is the Fermi velocity. We shall study the hydrodynamic regime, when

$$\omega\tau \ll 1 \qquad ql \ll 1 \tag{2.10}$$

where $\omega$ and $q$ are the angular frequency and the wavevector of a driving field, respectively. Lastly, solutions of the transport equations will be given here only for the case of the sharp resonance, when

$$\eta^2 \ll \omega_s\tau. \tag{2.11}$$

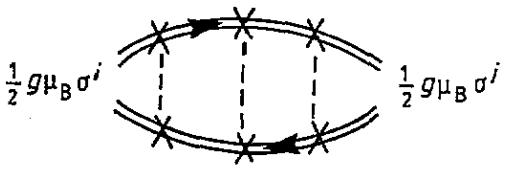


**Figure 1.** A typical diagram for the paramagnetic susceptibility $\chi_{ij}(\omega, q)$.

Consider the paramagnetic susceptibility $\chi_{ij}(\omega, q)$ of the system. To evaluate $\chi_{ij}(\omega, q)$, one should sum the so-called ladder diagrams one of which is shown in figure 1, where the broken line between two crosses corresponds to the factor $(m\tau)^{-1}$ and the double full curve represents the full impurity-averaged one-particle Green function

$$G^{R(A)}(\zeta, p, B) = [\zeta - H_0(p) + \mu \cdot B \pm i/2\tau]^{-1}. \tag{2.12}$$

Here the superscript R(A) stands for the retarded (advanced) part of the function. After the analytic continuation of the Green functions away from the discrete points on which they were originally defined to the space of two complex variables $\zeta$ and $\omega$, and the conversion

of the sum over discrete frequencies into a contour integral, one obtains, as is well known [19,20], three terms. The electron Green functions of the former two terms are both retarded or advanced. The influence of impurities on the terms is negligible in the limit (2.9). Therefore these terms yield the usual static Pauli susceptibility $\chi_{ij}(0,0)$ under the conditions (2.9) and (2.10):

$$\chi_{ij}(0,0) = \delta_{ij}\chi_P \qquad \chi_P = (m/\pi)(g\mu_B/2)^2. \tag{2.13}$$

The CESR contributes only to the latter term which includes one retarded and one advanced Green function. At temperatures much lower than the Fermi temperature $T_F = k_F^2/2mk_B$ ($k_B$ is the Boltzmann constant) this term may be represented as

$$\chi_{ij}^{res}(\omega, q) = \left(\frac{g}{2}\mu_B\right)^2 \frac{\omega}{2\pi i}\int \frac{d^2p}{(2\pi)^2} \times \mathrm{Tr}\left[G^A\left(\epsilon_F, p - \frac{q}{2}, B\right)\Sigma^i(\omega, q, B; p)G^R\left(\epsilon_F + \omega, p + \frac{q}{2}, B\right)\sigma^j\right] \tag{2.14}$$

where $\Sigma^i(\omega, q, B; p)$ is the impurity renormalized spin vertex. The matrix character of all quantities is understood. The Bethe–Salpeter equation for $\Sigma^i_{\alpha\beta}(\omega, q, B; p)$ plays the role of a quantum transport (kinetic) equation. It is schematically shown in figure 2.

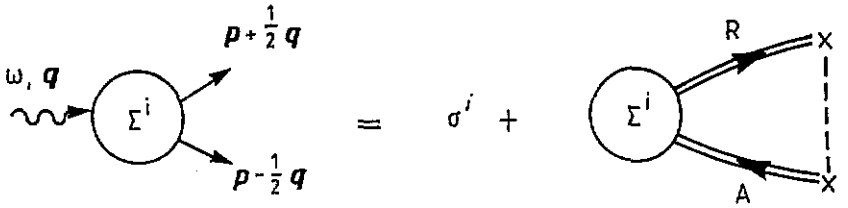


**Figure 2.** The Bethe–Salpeter equation for the renormalized spin vertex $\Sigma^i(\omega, q, B)$.

Further, in view of the inequalities (2.6) and (2.10) one can consider the Zeeman energy $H_Z = -\mu \cdot B$ and the Doppler energy $H_D = q \cdot v(p)/2$, entering into the Green functions

$$G^{R(A)}(\zeta, p \pm q/2, B) \simeq [\zeta - H_0(p) \mp q \cdot v(p)/2 + \mu \cdot B \pm i/2\tau]^{-1} \tag{2.15}$$

of equation (2.14), as small perturbations. Note that the velocity operator of the system

$$v(p) = i[H_0(p), r] = p/m + \alpha(c \times \sigma) \tag{2.16}$$

as well as the usual scalar part also has a spin component. The graphic representation of an expansion of $G(\zeta, p \pm q/2, B)$ in powers of $H_Z$ and $H_D$ can be found in figure 3. The unperturbed (bare) Green function (single full line in the diagrams) has the form

$$G^{R(A)}_{0,\alpha\beta}(\zeta, p) = [\zeta - H_0(p) \pm i/2\tau]^{-1}_{\alpha\beta} = \sum_{\nu=\pm} \Pi^{(\nu)}_{\alpha\beta}(p) G^{R(A)}_{(\nu)}(\zeta, p) \tag{2.17}$$

where

$$G^{R(A)}_{(\nu)}(\zeta, p) = [\zeta - E_{(\nu)}(p) \pm i/2\tau]^{-1} \qquad \nu = +, - \tag{2.18}$$

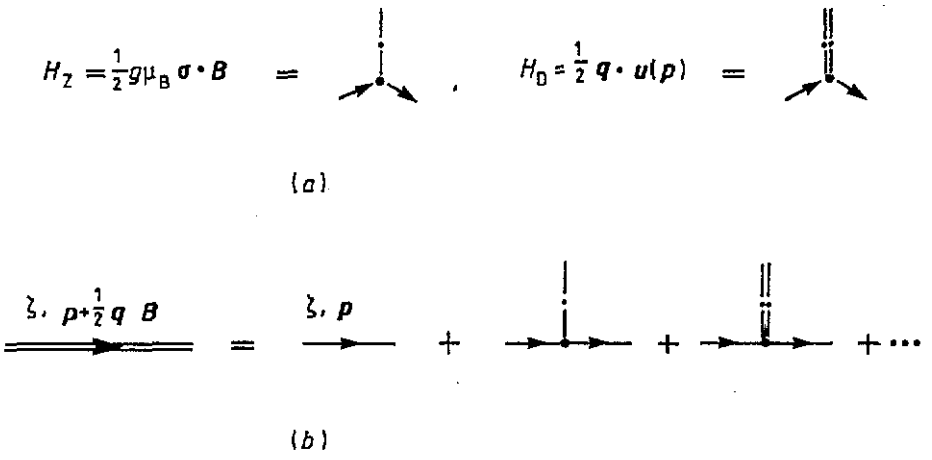


**Figure 3.** (*a*) Graphical representation of the Zeeman and Doppler energies. (*b*) The perturbation expansion of the full Green function.

and

$$E_{(\pm)}(p) = p^2/2m \pm \alpha p. \tag{2.19}$$

Here $E_{(\pm)}$ are the energies of two branches of the energy spectrum of $H_0(p)$ of positive and negative helicities (the projection of a spin on the $p \times c$ direction), and

$$\Pi^{(\pm)}(p) = \tfrac{1}{2}[1 \pm (\hat{p} \times c) \cdot \sigma] \tag{2.20}$$

are the projection operators on these branches. The difference between the diagram technique derived and the standard method [19,20] consists of the spinor structure of the bare Green function $G_0(\zeta, p)$ and the changed form of the velocity operator $v(p)$.

## 3. Transport equation

Consider the transport equation in figure 2. Owing to the short-ranged character of the impurity potential (2.4) every term of the diagrammatic expansion of figure 2 and, hence, the whole vertex function $\Sigma^i(\omega, q, B; p)$ actually does not depend on the momentum $p$. This property of the impurity potential enables one to perform the integration over internal momenta of each graph and to present the graphical equation of figure 2 in the form of a linear matrix equation

$$\Sigma^i_{\alpha\lambda}(\omega, q, B) = \sigma^i_{\alpha\lambda} + \Sigma^i_{\beta\gamma}(\omega, q, B)(\gamma\beta|T(\omega, q, B)|\alpha\lambda) \tag{3.1}$$

where the kernel function $T(\omega, q, B)$ is defined as shown in figure 4 and the summation convention for repeated indices is used.

The kernel $T(\omega, q, B)$ (the spinor indices are understood) has to be calculated to the first order in $\omega_s\tau$ and to the second order in $ql$:

$$T(\omega, q, B) \simeq T_0 + T(\omega) + T_1(B) + T_1(q) + T_2(q) \tag{3.2}$$

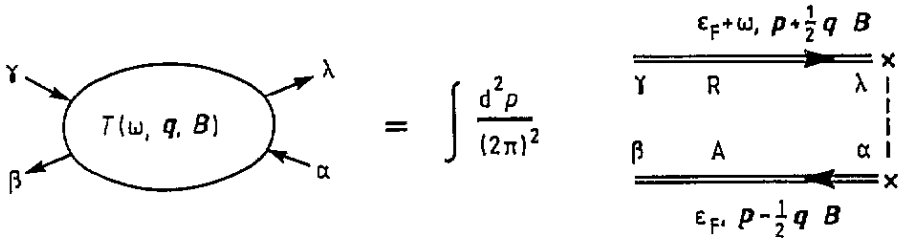


**Figure 4.** The kernel of the Bethe–Salpeter equation.

where the dependence of $T_1(\boldsymbol{B})$, $T_1(\boldsymbol{q})$ and $T_2(\boldsymbol{q})$ on $\omega$ can be dropped in the limit (2.10). A calculation (see appendix 2) yields the approximate expressions

$$(\gamma\beta|T(\omega)|\alpha\lambda) = \tfrac{1}{2}w\delta_{\gamma\beta}\delta_{\alpha\lambda} + \tfrac{1}{2}u(\boldsymbol{c}\cdot\boldsymbol{\sigma})_{\gamma\beta}(\boldsymbol{c}\cdot\boldsymbol{\sigma})_{\alpha\lambda} + \tfrac{1}{2}v(\boldsymbol{c}\times\boldsymbol{\sigma})^n_{\gamma\beta}(\boldsymbol{c}\times\boldsymbol{\sigma})^n_{\alpha\lambda} \tag{3.3}$$

$$(\gamma\beta|T_1(\boldsymbol{B})|\alpha\lambda) = -(g/|g|)\Omega e_{ijk}h^i\sigma^j_{\gamma\beta}\sigma^k_{\alpha\lambda} \tag{3.4}$$

$$(\gamma\beta|T_1(\boldsymbol{q})|\alpha\lambda) = \tfrac{1}{2}\mathrm{i}\eta Q e_{ijk}(\hat{\boldsymbol{q}}\times\boldsymbol{c})^i\sigma^j_{\gamma\beta}\sigma^k_{\alpha\lambda} \tag{3.5}$$

$$(\gamma\beta|T_2(\boldsymbol{q})|\alpha\lambda) = -\tfrac{1}{4}Q^2[\delta_{\gamma\beta}\delta_{\alpha\lambda} + (\boldsymbol{c}\cdot\boldsymbol{\sigma})_{\gamma\beta}(\boldsymbol{c}\cdot\boldsymbol{\sigma})_{\alpha\lambda} + (\boldsymbol{c}\times\boldsymbol{\sigma})^n_{\gamma\beta}\cdot(\boldsymbol{c}\times\boldsymbol{\sigma})^n_{\alpha\lambda}] \tag{3.6}$$

where

$$w = 1/(1-\mathrm{i}\omega\tau) \qquad u = (1-\mathrm{i}\omega\tau)/[(1-\mathrm{i}\omega\tau)^2+\eta^2] \qquad v = \tfrac{1}{2}(u+v) \tag{3.7}$$

$$\boldsymbol{h} = \boldsymbol{B}/B \qquad \Omega = \omega_s\tau \qquad Q = ql \tag{3.8}$$

The indices $i, j, k, n$ refer to the 3D vector Cartesian components (with a summation convention) and $e_{ijk}$ is the 3D antisymmetric tensor. In writing equations (3.3)–(3.6) we retained only leading terms in the parameter $\eta$. A diamagnetic contribution to $T_1(\boldsymbol{B})$ can be shown to include apart from $\omega_c\tau$ the additional small parameter $\eta^2$ and therefore is omitted. A contribution $H_2(\boldsymbol{q}, \boldsymbol{B})$ to the expansion (3.2) bilinear in $\boldsymbol{q}$ and $\boldsymbol{B}$ also exists. However, its effect on final results is negligible under the conditions (2.5)–(2.10). This assertion seems strange, since the aim of the paper is just to evaluate a contribution to the spin relaxation rate bilinear in the wavevector $\boldsymbol{q}$ and the field $\boldsymbol{B}$. Nevertheless, its correctness may be understood without any calculations. It is known that for $\boldsymbol{B} = \boldsymbol{q} = \boldsymbol{0}$ the sum of the impurity-ladder graphs for the case of the Fermi gas without SO coupling has the so-called diffusion pole $(\omega\tau)^{-1}$. By taking into account the SO interaction (1.1), but still for $\boldsymbol{B} = \boldsymbol{q} = \boldsymbol{0}$, the pole shifts into the lower complex half-plane $\omega \to \omega + \mathrm{i}/\tau_s$. So the sum of the 'single' ladder graphs (the ladder of the single-electron lines) can reach an amount of the order of $\tau_s/\tau \simeq \eta^{-2} \gg 1$. Therefore, it is clear that the main contribution to the problem under consideration comes from graphs which have the 'single' ladder between any two $H_Z$ and $H_D$ vertexes.

One should pay attention to the spinor structure of equations (3.3)–(3.6). Comparing the original expression of the kernel function $T(\omega, \boldsymbol{q}, \boldsymbol{B})$, as defined in figure 4, with the right-hand sides of equations (3.3)–(3.6), one can observe an important difference. Originally the kernel $T(\omega, \boldsymbol{q}, \boldsymbol{B})$ included, apart from the $p$ integral, the tensor product of two Green functions $G^R_{\gamma\lambda}G^A_{\alpha\beta}$. Unlike this, every term in equations (3.3)–(3.6) is the tensor product of a matrix which depends only on the indices $(\gamma, \beta)$ entering the graph in figure 4 from the left

and a matrix which depends only on the right-hand side indices $(\alpha, \lambda)$. This rearrangement of the spinor indices appears to be possible owing to identities for the tensor products of the Pauli matrices presented in the appendix 1.

Further, from equations (3.4) and (3.5) it is seen that the combination $\frac{1}{2}i\eta v_F(\boldsymbol{q} \times \boldsymbol{c})$ in the expression for the kernel $T_1(\boldsymbol{q})$ plays the same role as the magnetic field $\boldsymbol{B}$ does in $T_1(\boldsymbol{B})$. As the kernel $T_1(\boldsymbol{B})$ describes the well known Larmor precession of an electron spin about $\boldsymbol{B}$, a process induced by the kernel $T_1(\boldsymbol{q})$ could be interpreted as a spin rotation around the $\boldsymbol{q} \times \boldsymbol{c}$ axis or a spin precession induced by electron diffusion. The interpretation is not quite perfect. In particular, the Larmor precession is a pure dynamic process, whereas the kernel $T_1(\boldsymbol{q})$ is mainly associated with dissipation.

It is convenient to solve the transport equation (3.1) for every spin component $\boldsymbol{c} \cdot \boldsymbol{\sigma}$ and $\boldsymbol{c} \times \boldsymbol{\sigma}$ separately. Let $\Gamma_{\boldsymbol{c}\cdot\boldsymbol{\sigma}}$ and $\boldsymbol{\Gamma}_{\boldsymbol{c}\times\boldsymbol{\sigma}}$ be renormalized vertices corresponding to the bare vertices $\boldsymbol{c} \cdot \boldsymbol{\sigma}$ and $\boldsymbol{c} \times \boldsymbol{\sigma}$. For the former vertex, one can look for a solution of equation (3.1):

$$(\Gamma_{\boldsymbol{c}\cdot\boldsymbol{\sigma}})_{\alpha\lambda} = \boldsymbol{c} \cdot \boldsymbol{\sigma}_{\alpha\lambda} + (\Gamma_{\boldsymbol{c}\cdot\boldsymbol{\sigma}})_{\beta\gamma}(\gamma\beta|T(\omega, \boldsymbol{q}, \boldsymbol{B})|\alpha\lambda) \tag{3.9}$$

of the form

$$\Gamma_{\boldsymbol{c}\cdot\boldsymbol{\sigma}} = D\boldsymbol{c} \cdot \boldsymbol{\sigma} + \boldsymbol{V} \cdot (\boldsymbol{c} \times \boldsymbol{\sigma}) \tag{3.10}$$

which is none other than an expansion of the matrix $\Gamma_{\boldsymbol{c}\cdot\boldsymbol{\sigma}}$ in terms of the complete set of $2 \times 2$ matrices $(I, \sigma^x, \sigma^y, \sigma^z)$. A term proportional to the unit matrix, as one can verify, equals zero. Substituting (3.10) into equation (3.9) and using the expansion (3.2) and equations (3.3)–(3.6) one obtains a linear equation system, determining the scalar function $D(\omega, \boldsymbol{q}, \boldsymbol{B})$ and 2D vector function $\boldsymbol{V}(\omega, \boldsymbol{q}, \boldsymbol{B})$ of the form

$$\begin{aligned} D &= 1 + (u - \tfrac{1}{2}Q^2)\mathbf{D} + (\Omega\boldsymbol{h}' - i\eta Q\hat{\boldsymbol{q}} \times \boldsymbol{c}) \cdot \boldsymbol{V} \\ \boldsymbol{V} &= (\Omega\boldsymbol{h}' - i\eta Q\hat{\boldsymbol{q}} \times \boldsymbol{c})\mathbf{D} + (v - \tfrac{1}{2}Q^2)\boldsymbol{V} + \Omega(\boldsymbol{c} \cdot \boldsymbol{h})\boldsymbol{V} \times \boldsymbol{c} \end{aligned} \tag{3.11}$$

where

$$\boldsymbol{h}' = \boldsymbol{h} - \boldsymbol{c}(\boldsymbol{c} \cdot \boldsymbol{h}). \tag{3.12}$$

A solution of the system can be easily found by linear algebra methods and has the form (brief directions are given in appendix 3)

$$\begin{aligned} D &\simeq \tfrac{1}{2}i[1 - (\boldsymbol{c} \cdot \boldsymbol{h})^2][1/(z - z_+) + 1/(z - z_-)] \\ \boldsymbol{V} &\simeq [\boldsymbol{h}' + i(\boldsymbol{c} \cdot \boldsymbol{h})\boldsymbol{h} \times \boldsymbol{c}]/2(z - z_+) - [\boldsymbol{h}' - i(\boldsymbol{c} \cdot \boldsymbol{h})\boldsymbol{h} \times \boldsymbol{c}]/2(z - z_-) \end{aligned} \tag{3.13}$$

where

$$z = \omega\tau \qquad z_\pm = \pm\Omega - i\Gamma_\pm \qquad \Gamma_\pm = \tfrac{1}{4}\eta^2[3 - (\boldsymbol{c} \cdot \boldsymbol{h})^2] + \tfrac{1}{2}Q^2 \pm \eta Q\hat{\boldsymbol{q}} \cdot (\boldsymbol{c} \times \boldsymbol{h}). \tag{3.14}$$

Apart from the conditions (2.5)–(2.10), which are assumed to be fulfilled, there is an additional restriction for the applicability of equations (3.13). These expressions correctly represent the solution of equations (3.11) only in intervals near the resonance frequences $\pm\omega_s$ of the order of $\tau_s^{-1}(\boldsymbol{q}, \boldsymbol{B})$. In particular, they are not valid in the static limit $\omega = 0$. Therefore, equations (3.13) are somewhat symbolic; in the indicated vicinity of one pole the contribution of the other pole has to be omitted. We retain the contributions of both

the poles for convenience of application to the spin-flip Raman scattering mentioned in the introduction. In that case the pole at $\omega = \omega_s$ corresponds to the Stokes process and the pole at $\omega = -\omega_s$ corresponds to the anti-Stokes process.

Quite analogously, a solution of the transport equation for the vertex $\Gamma_{c\times\sigma}$, namely

$$(\Gamma_{c\times\sigma})_{\alpha\lambda} = c \times \sigma_{\alpha\lambda} + (\Gamma_{c\times\sigma})_{\beta\gamma}(\gamma\beta|T(\omega, q, B)|\alpha\lambda) \tag{3.15}$$

can be sought in the form

$$\Gamma^i_{c\times\sigma} = A^i c\cdot\sigma + W^{ij}(c\times\sigma)^j \qquad i, j = 1, 2. \tag{3.16}$$

The substitution (3.16) into equation (3.15) yields the linear equation system for the 2D vector $A(\omega, q, B)$ and the $2\times 2$ matrix $W^{ij}(\omega, q, B)$:

$$\begin{aligned} A^i &= (u - \tfrac{1}{2}Q^2)A^i + W^{ij}[\Omega h' - i\eta Q(\hat{q}\times c)]^j \\ W^{in} &= \delta^{in} - A^i[\Omega h' - i\eta Q(\hat{q}\times c)]^n + W^{ij}[(v - \tfrac{1}{2}Q^2)\delta^{jn} + \Omega(c\cdot h)e^{imn}c^m] \end{aligned} \tag{3.17}$$

where $\delta^{ij}$ is the Kronecker symbol. The solution of equations (3.17) has the form (appendix 3)

$$\begin{aligned} A^i &\simeq \tfrac{1}{2}\{-[h'^i - i(c\cdot h)(h\times c)^i]/(z - z_+) + [h'^i + i(c\cdot h)(h\times c)^i]/(z - z_-)\} \\ W^{ij} &\simeq \tfrac{1}{2}i\{[\delta^{ij} - (c\times h)^i\cdot(c\times h)^j - ie^{ijn}c^n(c\cdot h)]/(z - z_+) \\ &\quad + [\delta^{ij} - (c\times h)^i\cdot(c\times h)^j + ie^{ijn}c^n(c\cdot h)]/(z - z_-)\}. \end{aligned} \tag{3.18}$$

All the above discussion concerning the applicability of equations (3.13) has also to hold for equations (3.18).

It is important to realize the physical reason which does not allow the solution of the transport equation (3.1) to have a simple Bloch-type form (i.e. to have one pole of the first order) because of the restrictions mentioned above. Because of the SO energy (1.1) the operator of the total electron spin does not commute with the total Hamiltonian even in the absence of impurities and the external magnetic field. Of course, for an electron alone, having a momentum $p$, the projection of its spin on the $p\times c$ direction is conserved, but none of the components of the total spin is conserved. In other words, there is quantum fluctuation of the spin density in the ground state, which is one of the main features of the system under consideration. Spin dynamics to a high degree depend on whether the characteristic frequency $\alpha p_F$ of the fluctuations are less or more than the impurity broadening $\tau^{-1}$. From all that has just been said, one could conclude that the transport equation (3.1) hardly has a solution of the Bloch form. Nevertheless, in the dirty limit (2.8) merely examined in this paper a solution of such a form does exist, although only inside the narrow vicinities of the resonance frequencies. One should expect an even greater departure from the Bloch-type form in the clean limit $\alpha p_F\tau \geqslant 1$, where the role of the quantum spin fluctuations is expected to be very important.

## 4. The paramagnetic susceptibility

We now turn to an evaluation of the resonance part of the paramagnetic susceptibility tensor $\chi^{res}_{ij}(\omega, q, B)$ given by equation (2.14). In the leading approximation, one can set

$\boldsymbol{B} = \boldsymbol{q} = \boldsymbol{0}$ in the Green functions of equation (2.14), i.e. one can use the bare Green functions $G^0(\epsilon, \boldsymbol{p})$ instead of the full Green functions. The identity

$$\boldsymbol{\sigma} = \boldsymbol{c}(\boldsymbol{c} \cdot \boldsymbol{\sigma}) - \boldsymbol{c} \times (\boldsymbol{c} \times \boldsymbol{\sigma}) \tag{4.1}$$

permits us to express the vertex $\boldsymbol{\Sigma}$ of figure 2 in terms of the dressed vertices $\boldsymbol{\Gamma}_{\boldsymbol{c}\cdot\boldsymbol{\sigma}}$ and $\boldsymbol{\Gamma}_{\boldsymbol{c}\times\boldsymbol{\sigma}}$ as follows:

$$\boldsymbol{\Sigma} = \boldsymbol{c}\boldsymbol{\Gamma}_{\boldsymbol{c}\cdot\boldsymbol{\sigma}} - \boldsymbol{c} \times \boldsymbol{\Gamma}_{\boldsymbol{c}\times\boldsymbol{\sigma}}. \tag{4.2}$$

Now we have everything ready to calculate the right-hand side of equation (2.14):

(i) The bare Green functions are given by equation (2.17).

(ii) The dressed vertex $\boldsymbol{\Sigma}$ is given by equation (4.2), into which one should substitute equations (3.10) and (3.16) for the dressed spin vertices $\boldsymbol{\Gamma}_{\boldsymbol{c}\cdot\boldsymbol{\sigma}}$ and $\boldsymbol{\Gamma}_{\boldsymbol{c}\times\boldsymbol{\sigma}}$.

Then, substituting equations (4.2) and (2.17) into equation (2.13) and performing the integration over momentum and sum over spins, one finds that

$$\chi_{ij}^{\mathrm{res}}(\omega, \boldsymbol{q}, \boldsymbol{B}) \simeq -(\omega m/2\pi)(g\mu_{\mathrm{B}}/2)^2\{(\delta^{ij} - h^i h^j - \mathrm{i}e^{ijn}h^n)/[\omega - \omega_{\mathrm{s}} + \mathrm{i}\tau_{\mathrm{s},+}^{-1}(\boldsymbol{q})] + (\delta^{ij} - h^i h^j + \mathrm{i}e^{ijn}h^n)/[\omega + \omega_{\mathrm{s}} + \mathrm{i}\tau_{\mathrm{s},-}^{-1}(\boldsymbol{q})]\} \tag{4.3}$$

where

$$1/\tau_{\mathrm{s},\pm}(\boldsymbol{q}) = (1/\tau)\{\tfrac{1}{4}\eta^2[3 - (\boldsymbol{c} \cdot \boldsymbol{h})^2] + \tfrac{1}{2}Q^2 \pm \eta \boldsymbol{q} \cdot (\boldsymbol{c} \times \boldsymbol{h})\}. \tag{4.4}$$

The intensity (the differential cross section) for the spin-flip light scattering from $\omega_{\mathrm{I}}, \boldsymbol{k}_{\mathrm{I}}$ to $\omega_{\mathrm{S}}, \boldsymbol{k}_{\mathrm{S}}$ can be written as [16, 17]

$$\mathrm{d}^2\sigma/(\mathrm{d}\Omega\,\mathrm{d}\omega) \simeq [1 - \exp(-\omega/k_{\mathrm{B}}T)]^{-1}\mathrm{Im}[\nu_i \chi_{ij}^{\mathrm{res}}(\omega, \boldsymbol{q}, \boldsymbol{B})\nu_j] \tag{4.5}$$

where $\omega = \omega_{\mathrm{I}} - \omega_{\mathrm{S}}$, $\boldsymbol{q} = \boldsymbol{k}_{\mathrm{I}} - \boldsymbol{k}_{\mathrm{S}}$, $\boldsymbol{\nu} = (\boldsymbol{k}_{\mathrm{I}} \times \boldsymbol{k}_{\mathrm{S}})/|\boldsymbol{k}_{\mathrm{I}} \times \boldsymbol{k}_{\mathrm{S}}|$. Thus, the line shape of light scattering has the form

$$\mathrm{d}^2\sigma/(\mathrm{d}\Omega\,\mathrm{d}\omega) \simeq [1 - (\boldsymbol{\nu} \cdot \boldsymbol{h})^2][[\{\omega[1 + n_{\mathrm{B}}(\omega)]\tau_{\mathrm{s},+}^{-1}(\boldsymbol{q})\}/[(\omega - \omega_{\mathrm{s}})^2 + \tau_{\mathrm{s},+}^{-2}(\boldsymbol{q})] - [\omega n_{\mathrm{B}}(-\omega)\tau_{\mathrm{s},-}^{-1}(\boldsymbol{q})]/[(\omega + \omega_{\mathrm{s}})^2 + \tau_{\mathrm{s},-}^{-2}(\boldsymbol{q})]]] \tag{4.6}$$

where $n_{\mathrm{B}}(\omega) = [\exp(\omega/k_{\mathrm{B}}T) - 1]^{-1}$. Discussion of a pre-factor in equation (4.6) can be found in [16, 17].

## 5. Summary

We shall conclude by commenting on the results presented and raising questions for further investigations. We have studied the spin relaxation in the 2D electronic system with band SO coupling caused by the lack of 'up–down' symmetry. The main features of the CESR exhibited by equations (4.3) and (4.6) are as follows:

(i) the dependence of the uniform relaxation time on the angle between the applied magnetic field and the normal to the layer and

(ii) the anomalous space dispersion of the relaxation rate.

The best hope for experimental confirmation of these results seems to be in the line shape of the spin-flip Raman scattering.

Further, the method developed in this paper is well suited to treating the short-ranged impurity potential. It has permitted us to solve the kinetic problem without finding an explicit form of the distribution function (the density matrix) in momentum space. However, for the case of semiconductor structures it is desirable to have the possibility of treating other partial impurity-scattering amplitudes equally with the s wave. This is because the difference between the transport cross section and the full cross section may be rather large, especially in structures of high mobility. This much more difficult problem can probably be solved as well, although by slightly different methods. A similar calculation taking into account the diamagnetic quantization is also planned for the future.

## Appendix 1

In this appendix, a list of simply verified identities for the tensor products of the Pauli matrices used in the main text is presented. These identities are as follows:

$$\delta_{\alpha\beta}\delta_{\gamma\lambda} = \tfrac{1}{2}[\delta_{\gamma\beta}\delta_{\alpha\lambda} + (\boldsymbol{c}\cdot\boldsymbol{\sigma})_{\gamma\beta}(\boldsymbol{c}\cdot\boldsymbol{\sigma})_{\alpha\lambda} + (\boldsymbol{c}\times\boldsymbol{\sigma})^n_{\gamma\beta}(\boldsymbol{c}\times\boldsymbol{\sigma})^n_{\alpha\lambda}] \tag{A1.1}$$

$$(\boldsymbol{c}\times\boldsymbol{\sigma})^n_{\alpha\beta}(\boldsymbol{c}\times\boldsymbol{\sigma})^n_{\gamma\lambda} = \delta_{\gamma\beta}\delta_{\alpha\lambda} - (\boldsymbol{c}\cdot\boldsymbol{\sigma})_{\gamma\beta}(\boldsymbol{c}\cdot\boldsymbol{\sigma})_{\alpha\lambda} \tag{A1.2}$$

$$(\boldsymbol{a}\cdot\boldsymbol{\sigma})_{\alpha\beta}\delta_{\gamma\lambda} + \delta_{\alpha\beta}(\boldsymbol{a}\cdot\boldsymbol{\sigma})_{\gamma\lambda} = (\boldsymbol{a}\cdot\boldsymbol{\sigma})_{\gamma\beta}\delta_{\alpha\lambda} + \delta_{\gamma\beta}(\boldsymbol{a}\cdot\boldsymbol{\sigma})_{\alpha\lambda} \tag{A1.3}$$

$$(\boldsymbol{a}\cdot\boldsymbol{\sigma})_{\alpha\beta}\delta_{\gamma\lambda} - \delta_{\alpha\beta}(\boldsymbol{a}\cdot\boldsymbol{\sigma})_{\gamma\lambda} = \mathrm{i}\boldsymbol{a}\cdot(\boldsymbol{\sigma}_{\gamma\beta}\times\boldsymbol{\sigma}_{\alpha\lambda}) \equiv \mathrm{i}e_{ijk}a^i\sigma^j_{\gamma\beta}\sigma^k_{\alpha\lambda} \tag{A1.4}$$

$$\begin{aligned}(\boldsymbol{a}\cdot\boldsymbol{\sigma})_{\alpha\beta}(\boldsymbol{b}\cdot\boldsymbol{\sigma})_{\gamma\lambda} + (\boldsymbol{b}\cdot\boldsymbol{\sigma})_{\alpha\beta}(\boldsymbol{a}\cdot\boldsymbol{\sigma})_{\gamma\lambda} + 2(\boldsymbol{a}\cdot\boldsymbol{b})\delta_{\alpha\beta}\delta_{\gamma\lambda}\\ = (\boldsymbol{a}\cdot\boldsymbol{\sigma})_{\gamma\beta}(\boldsymbol{b}\cdot\boldsymbol{\sigma})_{\alpha\lambda} + (\boldsymbol{b}\cdot\boldsymbol{\sigma})_{\gamma\beta}(\boldsymbol{a}\cdot\boldsymbol{\sigma})_{\alpha\lambda} + 2(\boldsymbol{a}\cdot\boldsymbol{b})\delta_{\gamma\beta}\delta_{\alpha\lambda}\end{aligned} \tag{A1.5}$$

$$(\boldsymbol{a}\cdot\boldsymbol{\sigma})_{\alpha\beta}(\boldsymbol{b}\cdot\boldsymbol{\sigma})_{\gamma\lambda} - (\boldsymbol{b}\cdot\boldsymbol{\sigma})_{\alpha\beta}(\boldsymbol{a}\cdot\boldsymbol{\sigma})_{\gamma\lambda} = -\mathrm{i}[(\boldsymbol{a}\times\boldsymbol{b})\cdot\boldsymbol{\sigma}_{\gamma\beta}\delta_{\alpha\lambda} - \delta_{\gamma\beta}(\boldsymbol{a}\times\boldsymbol{b})\cdot\boldsymbol{\sigma}_{\alpha\lambda}] \tag{A1.6}$$

where $\boldsymbol{a}$, $\boldsymbol{b}$ and $\boldsymbol{c}$ are any 3D vectors.

## Appendix 2

We shall show here how one can obtain equations (3.3)–(3.6). The graphical definition of the kernel $T(\omega, \boldsymbol{q}, \boldsymbol{B})$ is presented in figure 4. Each of the full Green functions can be expanded in the Doppler and Zeeman energies as shown in figure 3. The result in the diagram language has the form shown in figure A1. The evaluation of the diagrams can be carried out in a manner similar to that of the Feynman graphs evaluation in spinor electrodynamics. In the integrals over momentum space, one should change the Cartesian coordinates for polar coordinates. Then angular integration gives rise to a combination of Pauli matrices, and the remaining radial integration can be elementarily performed with the help of the theory of residues. In the last step, one should use the identities in appendix 1. We shall carry out the calculation in detail for the graphs in figures A1($a$) and A1($b$),

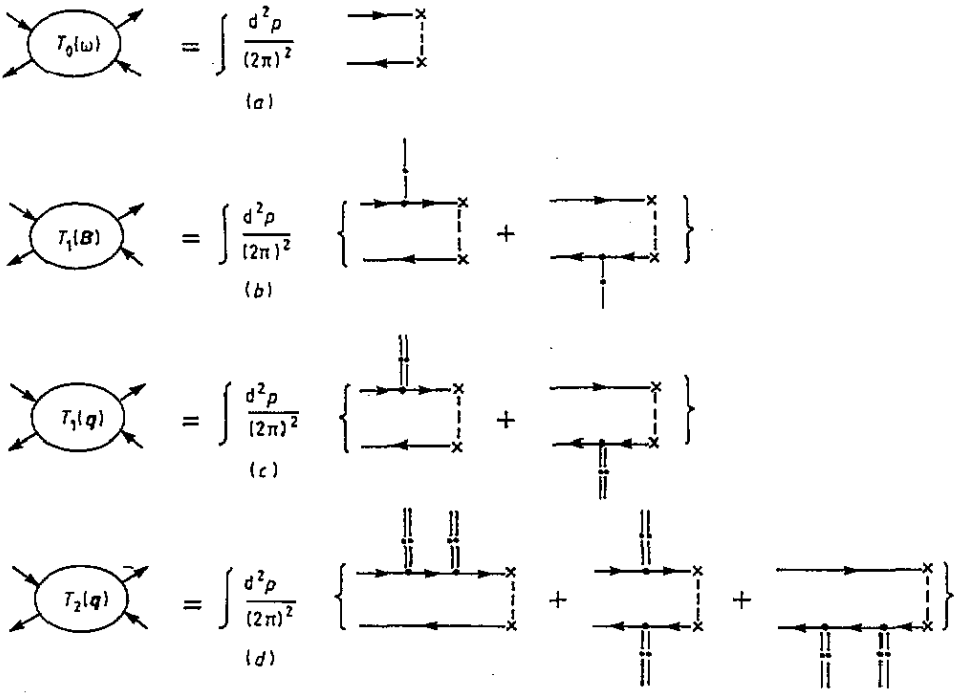


**Figure A1.** The perturbation expansion of the kernel function $T(\omega, q, B)$.

since the evaluation of the graphs in figures A1($c$) and A1($d$) is completely analogous, respectively, to that of the graphs in figures A1($a$) and A1($b$).

The contribution of the graph in figure A1($a$) taking into account equation (2.17) is given by

$$(\gamma\beta|T_0(\omega)|\alpha\lambda) = \frac{1}{m\tau}\int \frac{d^2p}{(2\pi)^2} G^{0(R)}_{\gamma\lambda}(\epsilon_F + \omega, p) G^{0(A)}_{\alpha\beta}(\epsilon_F, p) = \sum_{a,b=+,-} R_{(a,b)} Q_{(a,b)} \tag{A2.1}$$

where the indices in parentheses are the helicities of the electronic states and

$$R_{(a,b)} = \int \frac{d\hat{p}}{2\pi} \Pi^{(a)}_{\gamma\lambda}(p) \Pi^{(b)}_{\alpha\beta}(p) \tag{A2.2}$$

$$Q_{(a,b)} = \int \frac{d\xi}{2\pi\tau} G^{(R)}_{(a)}(\epsilon_F + \omega, p) G^{(A)}_{(b)}(\epsilon_F, p) \qquad \xi = \frac{p^2}{2m} - \epsilon_F. \tag{A2.3}$$

Substituting equation (2.20) into equation (A2.2), one obtains

$$\begin{aligned} R_{(a,b)} &= \tfrac{1}{4}\int \frac{dp}{2\pi}[\delta_{\gamma\lambda} + a(\hat{p}\times c)\cdot\sigma_{\gamma\lambda}][\delta_{\alpha\beta} + b(\hat{p}\times c)\cdot\sigma_{\alpha\beta}] \\ &= \tfrac{1}{4}[\delta_{\gamma\lambda}\delta_{\alpha\beta} + \tfrac{1}{2}ab(c\times\sigma)_{\gamma\lambda}(c\times\sigma)_{\alpha\beta}] \qquad a, b = +, -. \end{aligned} \tag{A2.4}$$

Substituting equations (2.18) and (2.19) into equation (A2.3), one obtains

$$Q_{(a,b)} \simeq \int \frac{d\xi}{2\pi\tau}\left(\omega - \xi - a\alpha p_F - \frac{i}{2\tau}\right)^{-1}\left(\xi - b\alpha p_F - \frac{i}{2\tau}\right)^{-1}. \tag{A2.5}$$

It follows from equation (A2.5) that

$$Q_{(++)} = Q_{(--)} = (1 - i\omega\tau)^{-1}$$
$$Q_{(+-)} = (1 - i\omega\tau + i\eta)^{-1} \qquad Q_{(-+)} = (1 - i\omega\tau - i\eta)^{-1}. \tag{A2.6}$$

Substituting equations (A2.4) and (A2.6) into equation (A2.1) one gets

$$(\gamma\beta|T_0(\omega)|\alpha\lambda) = \tfrac{1}{2}[\delta_{\gamma\lambda}\delta_{\alpha\beta} + \tfrac{1}{2}(c \times \sigma)^n_{\gamma\lambda}(c \times \sigma)^n_{\alpha\beta}][1/(1 - i\omega\tau)]$$
$$+ \tfrac{1}{2}[\delta_{\gamma\lambda}\delta_{\alpha\beta} - \tfrac{1}{2}(c \times \sigma)^n_{\gamma\lambda}(c \times \sigma)^n_{\alpha\beta}][(1 - i\omega\tau)/[(1 - i\omega\tau)^2 + \eta^2]. \tag{A2.7}$$

To obtain equation (3.3), one should use the identities (A1.1) and (A1.2).

The contribution of the graphs in figure A1($b$) can be evaluated to the leading order in the parameter $\eta$ setting the SO constant $\alpha$ equal to zero, i.e. substituting $G^0_{\alpha\beta}(\epsilon, p)$ for $g_{\alpha\beta}(\epsilon, p)$, where

$$g^{(R,A)}_{\alpha\beta}(\epsilon, p) = \delta_{\alpha\beta}(\epsilon - p^2/2m \pm i/2\tau)^{-1}. \tag{A2.8}$$

Then one obtains

$$(\gamma\beta|T(B)|\alpha\lambda) \simeq \frac{g\mu_B}{2m\tau}\int \frac{d^2p}{(2\pi)^2}\{[g^{(R)}(\epsilon_F, p)(\sigma \cdot B)g^{(R)}(\epsilon_F, p)]_{\gamma\lambda}g^{(A)}_{\alpha\beta}(\epsilon_F, p)$$
$$+ g^{(R)}_{\gamma\lambda}(\epsilon_F, p)[g^{(A)}(\epsilon_F, p)(\sigma \cdot B)g^{(A)}(\epsilon_F, p)]_{\alpha\beta}\}$$
$$= (g/|g|)\Omega i[\delta_{\gamma\lambda}(h \cdot \sigma)_{\alpha\beta} - \delta_{\alpha\beta}(h \cdot \sigma)_{\gamma\lambda}] \tag{A2.9}$$

which in view of the identity (A1.4) coincides with the right-hand side of equation (3.4).

By evaluating the graphs in figure A1($d$) one can use the Green functions $g_{\alpha\beta}(\epsilon, p)$ as well.

## Appendix 3

In this appendix, directions for solving the linear equation systems (3.11) and (3.17) will be given.

Excluding the function $D$ from equations (3.11) we obtain the equation for the vector $V$:

$$(D^{ij} + e^{ijk}a^k)V^j = X^i \qquad i, j = 1, 2 \qquad k = 1, 2, 3 \tag{A3.1}$$

where

$$D^{ij} = \delta^{ij}(1 - u + \tfrac{1}{2}Q^2)(1 - v + \tfrac{1}{2}Q^2) + X^iX^j$$
$$X = -(\Omega h' - i\eta Q\hat{q} \times c) \tag{A3.2}$$
$$a = -c\Omega(c \cdot h)(1 - u + \tfrac{1}{2}Q^2).$$

An equation of similar type is obtained if one excludes the vector function $A$ from the system (3.17):

$$W^{in}(D^{nj} + e^{ijk}a^k) = (1 - u + \tfrac{1}{2}Q^2)\delta^{ij}. \tag{A3.3}$$

One can verify that

$$(D^{ij} + e^{ijk}a^k)^{-1} = [\mathbf{D}(\hat{\mathbf{D}}^{-1})^{ij} - e^{ijn}a^n]/(\mathbf{D} + |\boldsymbol{a}|^2) \qquad \mathbf{D} = \det D^{ij}. \tag{A3.4}$$

To obtain the explicit form of the matrix $\hat{\mathbf{D}}^{-1}$ we introduce the unit vector $e = \boldsymbol{h}'/[1-(\boldsymbol{c}\cdot\boldsymbol{h})^2]^{1/2}$. Then the identity

$$\delta^{ij} = c^i c^j + e^i e^j + (\boldsymbol{c}\times\boldsymbol{e})^i(\boldsymbol{c}\times\boldsymbol{e})^j \qquad i,j = 1,2,3 \tag{A3.5}$$

allows one to represent the vector $\boldsymbol{X}$ in the form

$$\boldsymbol{X} = -\boldsymbol{e}\{\Omega[1-(\boldsymbol{c}\cdot\boldsymbol{h})^2]^{1/2} - \mathrm{i}\eta Q\hat{\boldsymbol{q}}\cdot(\boldsymbol{c}\times\boldsymbol{e})\} - \mathrm{i}\eta Q(\boldsymbol{c}\times\boldsymbol{e})(\hat{\boldsymbol{q}}\cdot\boldsymbol{e}) \tag{A3.6}$$

and the whole matrix $D^{ij}$ in the form

$$D^{ij} = Ke^ie^j + M[e^i(\boldsymbol{c}\times\boldsymbol{e})^j + e^j(\boldsymbol{c}\times\boldsymbol{e})^i] + L(\boldsymbol{c}\times\boldsymbol{e})^i(\boldsymbol{c}\times\boldsymbol{e})^j \tag{A3.7}$$

where

$$\begin{aligned} K &= (1-u+\tfrac{1}{2}Q^2)(1-v+\tfrac{1}{2}Q^2) + \{\Omega[1-(\boldsymbol{c}\cdot\boldsymbol{h})^2]^{1/2} - \mathrm{i}\eta Q\hat{\boldsymbol{q}}\cdot(\boldsymbol{c}\times\boldsymbol{e})\} \\ M &= \mathrm{i}\eta Q(\hat{\boldsymbol{q}}\cdot\boldsymbol{e})\{\Omega[1-(\boldsymbol{c}\cdot\boldsymbol{h})^2]^{1/2} - \mathrm{i}\eta Q\hat{\boldsymbol{q}}\cdot(\boldsymbol{c}\times\boldsymbol{e})\} \\ L &= (1-u+\tfrac{1}{2}Q^2)(1-v+\tfrac{1}{2}Q^2) - \eta^2Q^2(\hat{\boldsymbol{q}}\cdot\boldsymbol{e})^2. \end{aligned} \tag{A3.8}$$

It is now evident that

$$\begin{aligned} (\hat{D}^{-1})^{ij} = (KL - M^2)^{-1}\{&Le^ie^j - M[e^i(\boldsymbol{c}\times\boldsymbol{e})^j + e^j(\boldsymbol{c}\times\boldsymbol{e})^i] \\ &+ K(\boldsymbol{c}\times\boldsymbol{e})^i(\boldsymbol{c}\times\boldsymbol{e})^j\}. \end{aligned} \tag{A3.9}$$

Equations (A3.4) and (A3.9) allow one to obtain the solution of equations (A3.1) and (A3.3) and, consequently, equations (3.11) and (3.17). All that remains for obtaining equations (3.13) and (3.18) is to simplify the expressions for the quantities $K$, $L$ and $\boldsymbol{a}$ using the inequalities (2.5)–(2.10).

## References


[1] Stein D, von Klitzing K and Weimann G 1983 *Phys. Rev. Lett.* **51** 130
[2] Bychkov Yu A and Rashba E I 1984 *J. Phys. C: Solid State Phys.* **17** 6039
[3] Lommer G, Malcher F and Rössler U 1988 *Phys. Rev. Lett.* **60** 728
[4] Dresselhaus P D, Papavassiliou C M A, Wheeler R G and Sacks R N 1992 *Phys. Rev. Lett.* **68** 106
[5] Das B, Datta S and Reifenberger R 1990 *Phys. Rev.* B **41** 9278
[6] Luo J, Munekata H, Fong F F and Stiles P J 1988 *Phys. Rev.* B **38** 10 142
[7] Romestain R, Geshwind S and Devlin G E 1977 *Phys. Rev. Lett.* **39** 1583
[8] Edelstein V M 1991 *Solid State Commun.* **77** 859
[9] Müller G, Weiss D, Khaetskii A V, von Klitzing K and Koch S 1992 *Phys. Rev.* B **45** 3932
[10] Elliott R J 1954 *Phys. Rev.* **96** 266
[11] Hirshfelder P J, Wolfle P and Einzel D 1988 *Phys. Rev.* B **37** 83
[12] Dyakonov M I and Perel' V I 1971 *Fiz. Tverd. Tela* **13** 3581 (Engl. Transl. 1972 *Sov. Phys.–Solid State* **13** 3023)
[13] Gross E F, Zakharchenya B P and Konstantinov O B 1961 *Fiz. Tverd. Tela* **3** 305 (Engl. Transl. 1961 *Sov. Phys.–Solid State* **3** 221)

[14] Hopfield J J and Thomas D G 1961 *Phys. Rev.* **122** 35
[15] White R M 1970 *Quantum Theory of Magnetism* (New York: McGraw-Hill)
[16] Abstreiter G, Cardona M and Pinczuk A 1984 *Light Scattering in Solids IV (Topics in Applied Physics 54)* ed M Cardona and G Gunterodt (Berlin: Springer) p 5
[17] Geshwind S and Romestain R 1984 *Light Scattering in Solids IV (Topics in Applied Physics 54)* ed M Cardona and G Gunterodt (Berlin: Springer) p 151
[18] Levitov L S, Nazarov Yu V and Eliashberg G M 1985 *Zh. Eksp. Teor. Fiz.* **88** 229 (Engl. Transl. 1985 *Sov. Phys.–JETP* **61** 170)
[19] Abrikosov A A, Gor'kov L P and Dzyaloshinskii I E **1863** *Methods of Quantum Field Theory in Statistical Physics* (Englewood Cliffs, NJ: Prentice-Hall)
[20] Siegel J 1969 *Phys. Rev.* **186** 182
[21] Barnes S E 1981 *Adv. Phys.* **30** 801